UNITED STATES
NUCLEAR REGULATORY COMMISSION
WASHINGTON, D.C. 20555-0001

SAFETY EVALUATION BY THE OFFICE OF NUCLEAR REACTOR REGULATION

PALISADES: PRESSURE VESSEL FLUENCE REEVALUATION

CONSUMERS POWER COMPANY

DOCKET NO. 50-255

1.0 SUMMARY

Detailed calculations of the Palisades pressure vessel and cavity fluence for Cycles 1-11 have been carried out. The calculations use a pin-wise fuel exposure-dependent description of the core neutron source, and plant design and operating data provided by the Consumers Power Company (CPC) and Westinghouse (W). The calculations employ the DORT (Reference 1) discrete ordinates particle transport code and the MESH (Reference 2) source integration code, together with the BUGLE-93 ENDF/B-VI cross section data. The models include the recent (Reference 3) revisions to the Palisades plant data including the reduced downcomer/bypass temperatures, updated cycle-dependent pin-wise source and the increased vessel diameter and thickness. The BNL calculations indicate a Cycle-11 ($E > 1$ MeV) vessel peak inner wall fluence of 1.60×10^{19} n/cm^2, compared to the CPC/W calculation (prior to the application of the 0.83 measurement bias) of 1.59×10^{19} n/cm^2. An evaluation of uncertainties indicates a one-sigma uncertainty in these predictions of about 14 percent.

In order to evaluate the CPC/W interpretation of the U-238 and Np-237 fission dosimeters, coupled neutron/photon transport calculations of the Palisades dosimeter photo-fission contribution were also performed. These calculations indicate that the photo-fission contribution to the U-238(n,f) vessel-wall and cavity dosimeters is 15 percent and 4 percent, respectively, compared to the CPC/W values of 11 percent and 4 percent. The photo-fission contribution to the Np-237(n,f) vessel-wall and cavity dosimeters is calculated to be 8 percent and 1 percent, respectively, compared with the CPC/W predictions of 7 percent and 1 percent.

A review of the CPC/W application of the in-vessel and cavity measurements to the determination of the Palisades best estimate fluence has also been performed. This review examined the Palisades measurement to calculation (M/C) data base and the determination of the bias in the calculated fluence. The review indicated that the M/C data is not uniform and that certain important data subsets exist for which the M/C calculational bias is significantly different than the M/C = 0.88 data-base average. The in-vessel high energy and low energy dosimeters indicate a substantial difference in M/C

ENCLOSURE 1

fluence bias; M/C = 1.0 ± .03 versus M/C = 0.86 ± .02, respectively. In the CPC/W analysis this difference is assumed to be due to a spectrum dependent error in the DORT calculations which results in an exact calculation above E > 4.0 MeV and an overprediction for E < 4.0 MeV. Based on this assumption, a 12 percent M/C fluence reduction is applied to the DORT E > 1.0 MeV fluence prediction. While this conclusion may be correct, several other possible explanations for the observed 1.00/0.86 difference between the high/low-energy M/C biases that would not require a reduction in the DORT calculated fluence are identified. These include: (1) the use of erroneously low dosimeter cross sections for Fe-54 and Ni-58 in the interpretation of the measurement, and/or (2) errors in the Fe-54 and Ni-58 measurements.

2.0 INTRODUCTION

Consumers Power Company provided the evaluation of the Palisades pressure vessel peak wall fluence (PWF) through Cycle-9 in Reference 4 (June 1993). The Brookhaven National Laboratory (BNL) evaluation of this analysis (Reference 5) concluded that the CPC/W prediction of the Palisades vessel PWF was conservative. In the recent CPC submittal of Reference 3 (April 1996) entitled, "Palisades Plant Updated Reactor Vessel Fluence Values," the Reference 4 (1993) analysis is updated to include recent modeling improvements and the Cycle 10 and 11 cavity measurements. This updated fluence analysis takes credit for certain modeling conservatisms (i.e., reduced downcomer temperature, increased vessel diameter and decreased neutron source) which amount to about 8 percent. In addition, determines the best estimate fluence value using a calculation to measurement bias of 17 percent. The bias consists of two parts: 12 percent due to the results of dosimetry and 5 percent due to spectral adjustments of the dosimetry measurements. The sum of these changes results in a 25 percent reduction in the predicted vessel fluence. The two parts of the proposed reduction differ in that the physical quantities on which the 8 percent is based result from direct measurements while the 17 percent bias is the result of dosimetry (indirect measurements), averaging and spectral adjustments.

In the present analysis, an independent evaluation of the Palisades Cycle-11 vessel PWF is performed. The primary focus of this evaluation is: (1) the plant and source modeling and calculation of the vessel fluence, (2) the contribution of photo-fission to the U-238 and Np-237 dosimeter fluence measurements, (3) the uncertainty in the predicted fluence, and (4) the application of the measurements in determining the Palisades best-estimate fluence. The plant and source modeling were selected for detailed review since several of the identified conservatisms included in the Reference 3 updated analysis concerned the calculational models. The U-238 and Np-237 dosimeter measurements are used to adjust the calculated fluence and, since the photo-fission contribution to these dosimeters includes a substantial uncertainty, a detailed analysis of the photo-fission response was also performed. The application of the measurements was reviewed because the measurement renormalization results in a substantial reduction (17 percent) in the fluence.

The methods used to calculate the vessel fluence and determine the dosimeter response in this analysis are consistent with the methods described in the

Draft Regulatory Guide DG-1053. In performing this analysis a substantial effort was made to insure the use of the latest ENDF/B-VI nuclear cross section and fission spectra data. The required plant operating and design data including: (1) the geometry and material compositions of the core, internals, vessel and cavity, (2) the cycle-dependent power and exposure distributions, (3) the operating temperatures, and (4) the parameter uncertainties were obtained from CPC/W. The BNL calculational models are based on the information provided by CPC in the initial submittal (Reference 3) and attached WCAP-14557 Westinghouse Report (Reference 6), and in the subsequent (References 8-11) CPC responses to the requests for additional information (RAIs) included in Reference 12. While these plant data were reviewed and generally found to be consistent and within expected limits, a detailed validation of the basic source data (e.g., verification of the temperature measurements, SIMULATE-3 depletion calculations and material composition specifications) was not performed.

The DORT discrete ordinates transport code was used to calculate the transport of the core neutron flux out to the vessel and into the cavity. The DORT calculations were performed for an axially averaged horizontal plane in (r,θ) geometry. The MESH code was used to determine the space-energy dependent core neutron source in the required (r,θ) geometry for input to DORT. The calculations made use of the recent update to the MESH code to allow an accurate modeling of the core pin-wise power and source distributions in the peripheral assemblies and the stainless steel pins included in Cycles 8, 10 and 11. Cycle-specific DORT calculations were performed for each cycle and then combined to determine the total accumulated vessel fluence through Cycle 11.

The calculational methods are described in the following Section 3, the vessel fluence analysis is given in Section 4, the evaluation of the photo-fission contribution is given in Section 5, and the evaluation of the application of the measurements to determine the best estimate fluence is described in Section 6.

3.0 CALCULATIONAL METHODOLOGY

3.1 Neutron Cross Sections and Fission Spectra

The Palisades fluence calculations were performed with the BUGLE-93, 47-group cross section library (Reference 13). The BUGLE-93 broad-group library was determined by collapsing the ENDF/B-VI VITAMIN-B6 171-group neutron/photon cross section set using spatially dependent spectra calculated for a typical PWR configuration. This library includes the recent updates to the iron, hydrogen, and oxygen cross sections, which together are known to result in a significant increase in the pressure vessel fluence prediction.

The fission spectra for U-235, U-238, Pu-239, Pu-240, Pu-241, and Pu-242 were used in the MESH calculations of the core neutron source. The ENDF/B-VI fission spectra for U-235, U-238, Pu-239, and Pu-241 were processed with NJOY (Reference 14). The surveillance capsule dosimeter reaction rates were calculated using ENDF/B-VI cross sections. The ENDF/B-VI dosimeter cross section data were collapsed to the 47 group structure using NJOY.

3.2 Core Neutron Source

The calculation of the core neutron source includes the effect of the strong pin-wise variations of the power distribution in the fuel assemblies located near the core boundary. The cycle dependent pin-wise power distribution for each assembly was provided in Reference 7. The MESH code was used to allocate the pin power to the individual (r,θ) mesh blocks. This allocation was performed by a numerical integration of the power distribution, defined on the (x,y) pin-wise mesh, over each (r,θ) mesh block. This numerical integration typically employed greater than 100 integration mesh points per fuel pin and was shown to be accurate to within 1 percent for each (r,θ) mesh block. As an example, the detailed core neutron source for Cycles 1 and 11 are given in Figures 1 and 2, respectively.

The magnitude of the core neutron source increases with fuel burnup due to the higher number of neutrons produced per MeV of energy by a Plutonium fission. This was taken into account by calculating the ν/κ [neutrons/MeV], using fuel burnup dependent isotopic fission fractions. In addition, the fission spectrum was also considered to be dependent on the fuel burnup in order to account for the harder more penetrating neutron spectrum characteristic of the Plutonium fissions in the high burnup fuel.

The group dependent pin-wise source for each fuel assembly was determined for each cycle and used in the cycle specific DORT calculations. The (r,θ) spatial mesh was modified in the MESH/DORT models to allow an accurate representation of the stainless steel pins that have been introduced in Cycles 8, 10 and 11 for flux reduction.

3.3 Neutron Transport Calculations

The neutron transport calculations were performed with the ORNL DORT discrete ordinates transport code using the 47 group BUGLE-93 library. The calculations were performed in a fixed source mode for a radial (r,θ) plane. The radial (r,θ) calculations were performed in a two step "boot strap" fashion in which an inner one-eighth 45°-azimuthal sector was first calculated. A second outer one-eighth core 45°-azimuthal sector was then calculated using the flux on the inner surface of the annulus, calculated in the first inner calculation, as an input boundary condition. A radial overlap of about 15 cm between the inner and outer calculational regions was maintained to insure that the neglect of the outer geometry in the inner problem had a negligible effect (less than 0.5%) on the vessel fluence calculations. The vessel axial peak was conservatively taken to be the same as the core axial power peak.

The calculations were performed using an S_8 quadrature and a P_3 angular decomposition of the scattering cross sections. The (r,θ) mesh included 61 angular mesh intervals, and 106 and 125 radial mesh intervals, respectively, in the inner and outer bootstrap calculations. The angular (θ) and radial (r) mesh densities were increased at material interfaces where the geometry was changing rapidly, and at the capsule locations.

Vacuum boundary conditions were used on the outer radial and axial boundaries of the problems, and reflecting boundary conditions were used on the internal $\theta = 0°$ and $\theta = 45°$ azimuthal boundaries. A pointwise flux convergence of 10^{-3} was used together with an integrated flux convergence criterion of 10^{-3}.

4.0 PALISADES VESSEL FLUENCE AND SURVEILLANCE CAPSULE ANALYSIS

4.1 Vessel Fluence Calculations

The pressure vessel peak wall fluence was calculated for each of the Palisades eleven operating cycles to account for the cycle dependent changes in the downcomer temperatures, and to allow the determination of the surveillance capsule cycle dependent reaction rates. The calculations include the increased vessel base metal thickness of 8.792 in., the increased vessel base metal inner radius of 86.35 in., the cycle specific bypass and inlet temperatures based on the plant monitoring data, and the updated cycle specific SIMULATE-3 pin-wise power distributions provided by CPC in Reference 4. The calculations include detailed modeling of the stainless steel replacement rods in the peripheral fuel assemblies as described in Reference 10, and the in-vessel surveillance capsule geometry as described in Reference 11.

The fluence was determined at the inner-wall of the vessel at the interface between the vessel clad and the base metal. The calculated fluence peak occurs at the 15.5° azimuth, opposite the corner assembly on the core flats. The calculated fluence is presented in Table 1 and indicates a peak $E > 1.0$ MeV of 1.60×10^{19} n/cm^2 at the vessel inner-wall at the end of Cycle 11. The fluence contribution and the cycle length (in effective full power days) for each cycle are also given in Table 1. For comparison, the W (Reference 6) prediction of the peak wall fluence accumulated through Cycle 11 is 1.59×10^{19} n/cm^2. (The comparison of cycle-specific fluences is not made since the cycle values were not reported in Reference 6.) This W fluence value does not include the 0.83 multiplicative adjustment that W applies to the calculated fluence to ensure agreement between the calculation and the Palisades measurements. This agreement between the BNL and W calculations (to within 1.0 percent) confirms the fluence prediction models and methods, and is well within the calculational uncertainties.

In order to estimate the uncertainty in the BNL $E > 1.0$ MeV fluence prediction, a series of sensitivity calculations were performed for the known sources of significant uncertainty. In Table 2, these sensitivities are given along with the estimated (one sigma) uncertainty components. The pressure vessel diameter uncertainty of ± 0.12 in. was provided by CPC (Reference 11). The 8 percent source uncertainty (Item 2) is based, in part, on an estimate of the uncertainty in the peripheral assembly powers, and the (Item 5) water temperature uncertainties are based on expected reactor coolant system temperature calculation/measurement uncertainties. The nuclear data uncertainty estimate (Item 3) is based on expected data uncertainties and the numerical procedures uncertainty (Item 4) is based on the sensitivity of the fluence to numerical modeling and solution approximations. The other uncertainties included in Item 6 are relatively small model uncertainties that combine to add an additional 5 percent uncertainty to the total fluence. The

total Palisades inner-wall E > 1.0 MeV fluence uncertainty estimate is ± 14 percent (1 σ).

4.2 Surveillance Capsule Calculations

In the CPC/W methodology, the best estimate fluence is determined by applying a multiplicative bias factor of 0.83 to the DORT calculation which results in a 17 percent reduction in the predicted fluence. This bias factor is based on a data base of calculation to measurement comparisons made for the Palisades in-vessel and cavity surveillance capsules. As part of the evaluation of this procedure, calculations of several Palisades in-vessel and cavity capsule measurements were performed. The capsules calculated include: (1) the W-290 in-vessel capsule located at the 20° azimuth which was withdrawn after Cycle 5, (2) the W110 in-vessel capsule located at the 20° azimuth which was withdrawn after Cycle 10, and (3) the three cavity capsules located at the 16° azimuth which were irradiated during Cycle 8, Cycle 9, and Cycles 10 and 11. The capsules were modeled in detail in the DORT calculations and were located at the positions given in Reference 6.

The reaction rates for these capsules were calculated for the Cu-63(n,α), Ti-46(n,p), Fe-54(n,p), Ni-58(n,p), U-238(n,f) and Np(n,f) reactions using the BUGLE-93 ENDF/B-VI dosimetry cross sections. The calculated reaction rates were compared to the CPC/W predictions for each capsule dosimeter and the results of this comparison are presented in Table 3. The agreement of the BNL and CPC/W predictions is generally good (to within a standard deviation of about five percent) and consistent with the good agreement observed between the E > 1.0 MeV vessel fluence calculations of Table 1.

5.0 EVALUATION OF THE PHOTO-FISSION CONTRIBUTION TO THE U-238(n,f) AND Np-237(n,f) DOSIMETERS

The WCAP-14557 treatment of the photo-fission contribution to the U-238(n,f) and Np-237(n,f) dosimeters results in a reduction in the neutron fluence inferred from these measurements. This fluence reduction contributes directly to the 17 percent reduction (i.e., the 0.83 bias factor) in the Palisades best estimate fluence. In view of the uncertainty associated with this contribution, a detailed analysis of the U-238 and Np-237 photo-fission effect was performed.

The determination of the photo-fission reaction requires the calculation of both the neutron and gamma flux. Since a significant fraction of the gamma flux is generated by low energy thermal neutron captures, a cross section library with a reliable thermal energy treatment is required. The CPC/W calculations were performed with the BUGLE-93 ENDF/B-VI cross section library which includes only two thermal neutron groups with no upscattering and is typically used for shielding applications rather than thermal neutron calculations. In order to provide an accurate treatment of the thermal neutron captures and a reliable gamma source, the MATXS12 ENDF/B-VI (Reference 15) coupled neutron/photon library was used for the calculation of the photo-fission contribution to the U-238 and Np-237 dosimeter responses. This cross section library is designed for light water thermal systems and

includes 42 thermal neutron groups and upscattering. For comparison, the calculations were also performed with the BUGLE-93 cross section library which was also used in the CPC/W calculations. The MATXS12 and BUGLE-93 (n,f) reaction rates were calculated using their respective dosimetry cross sections, and the U-238 and Np-237 photo-fission reaction rates were calculated using the cross sections of References 16 and 17, respectively.

The DORT coupled neutron/gamma transport calculations were performed using the detailed (r,θ) Palisades geometry. The results of these calculations are presented in Table 4 and indicate that the BUGLE-93 and MATXS12 predictions of the U-238(γ,f) and Np-237(γ,f) reaction rates are in good agreement for both the in-vessel and cavity capsules. The MATXS12 predictions are compared with the CPC/W predictions in Table 5 and indicate that the BNL and CPC/W photo-fission predictions are in good agreement. The comparisons indicate that: (1) the photo-fission correction is 15 percent and 4 percent for the U-238(n,f) dosimeter for the vessel inner-wall and cavity capsules, respectively, and (2) the photo-fission correction is eight percent and one percent for the Np-237 dosimeter for the vessel inner-wall and cavity capsules, respectively.

6.0 EVALUATION OF BEST-ESTIMATE FLUENCE DETERMINATION

6.1 Best-Estimate Fluence Determination

The best estimate fluence determination of WCAP-14557 is made using the Palisades in-vessel and cavity measurements data base. The Palisades measurements are compared to predictions of the dosimetry measurements made using the same codes and methods that are used to predict the vessel inner-wall fluence. Based on these M/C comparisons of the dosimeter reaction rates, a M/C bias of 12 (±7) percent is determined. This M/C bias is then adjusted using a least squares adjustment technique to account for uncertainties in the measurements and calculations. In the case of Palisades this adjustment increases the M/C bias from 12 percent to 17 percent, and implies the calculations are overpredicting the fluence by 17 percent. The determination of the M/C bias and the adjustment method are discussed in the following sections.

6.2 Fluence Calculation to Measurement Bias

The fluence M/C bias is based on the neutron dosimetry included in the accelerated surveillance capsule (A240) located on the outer-wall of the core support barrel, the three vessel inner-wall capsules (W290, W290-9 and W110), and the 13 cavity measurements. The accelerated capsule was withdrawn after two cycles, the inner-wall capsules, A290 and W110, were withdrawn after Cycles 5 and 10, respectively, and Capsule A290-9 was only irradiated for Cycle 9. The cavity dosimetry included three azimuthal measurements for Cycle 8, four measurements for Cycle 9, and five measurements which were

irradiated for both Cycles 10 and 11. All (except one) of the cavity measurements included the six dosimetry measurements; Cu-63(n,α), Ti-46(n,p), Fe-54(n,p), Ni-58 (n,p), U-238(n,f) and Np-237(n,f). The in-vessel dosimetry included all of these measurements except, in some cases, the U-238(n,f) and Np-237(n,f) dosimeters. The Palisades database included a total of 96 M/C comparisons.

The M/C database used to determine the 0.88 fluence bias has been reviewed with respect to the consistency and reliability of the M/C data. The review was based on the material included in WCAP-14557 and the responses to the RAIs of References 4 and 8-11. The review concerned the measurement database since the analysis of Sections 4 and 5 provided validation of the CPC/W fluence calculations. The primary focus was on: (1) the reliability of the M/C = 0.88 bias of Table 7.2-1, and (2) the applicability of this bias in determining a high confidence best estimate value for the Palisades vessel fluence.

It is first noted that while the database includes random uncertainties due to the measurement process, these uncertainties contribute to the variability in the comparisons and are generally accounted for by the indicated ± 0.072 (one standard deviation) uncertainty in the calculated bias. The data base included dosimeter reactions with product half lives ranging from about 70 days to about 30 years which provided sensitivity to both the recent (few months) and long term (Cycles 1-11) fuel loading and operating history. However, the data base did not indicate any significant dependence of the M/C bias on the dosimeter reaction half life.

The Table 7.2-1 database consists of six dosimeter types which are measured for four in-vessel capsules and 13 cavity capsules. The data base includes a total of 96 M/C values which are averaged to determine the 12 percent fluence bias. The averaging of this data assumes that the M/C values represent samples drawn from the same underlying population. However, an examination of the data indicates that there are several subsets of the M/C database which have different M/C biases and appear to represent different distributions. For example, the M/Cs for the in-vessel dosimeters with thresholds greater than 4.0 MeV (viz., Cu-63 and Ti-46) indicate an M/C bias of 1.0 ± .03. The M/Cs for the cavity dosimeters with thresholds greater than 4.0 MeV indicate an M/C bias of 0.91 ± .03, and suggest a basic difference between the in-vessel and cavity M/Cs for the high energy dosimeters. In addition, the cavity dosimeters with thresholds less than 4.0 MeV indicate an M/C bias of 0.85 ± .07. This difference is important since about 80 percent (77 out of 96) of the M/Cs are cavity measurements which yield the lowest fluence and, consequently, this database tends to maximize the fluence reduction.

The M/C bias indicates a significant dependence on the location of the dosimeters (cavity versus in-vessel) and on the energy threshold of the dosimeters ($E > 4.0$ MeV versus $E < 4.0$ MeV) as seen in Figures 3 and 4. In determining the measurement to calculation bias for the prediction of the inner wall vessel fluence, it is important to recognize the difference in the fluence spectrum at these two locations. In Figure 5, a comparison of the fluence spectrum at the location of the accelerated (barrel outer wall), the vessel inner wall and the cavity capsules is presented. It is evident from

this comparison that the fluence spectrum at the cavity capsule differs significantly from the spectrum at the vessel inner wall where the fluence prediction is required. This is due, in part, to the fact that Palisades does not have a thermal shield and the additional about 8 inches of steel between the inner wall and cavity locations. It is concluded that the M/C comparisons made for the in vessel dosimetry are a more accurate indication of the M/C comparisons made for the in vessel dosimetry are a more accurate indication of the M/C to be used for the in vessel fluence prediction.

From Figure 4, it is seen that the in vessel M/C bias is 1.00 ± .03 for the dosimeters with thresholds E > 4.0 MeV, and 0.86 ± .02 for the dosimeters with thresholds E < 4.0 MeV. In the CPC/W analysis this difference is assumed to be due to a spectrum dependent error in the DORT calculations which results in an exact calculation above E > 4.0 MeV and an overprediction for E < 4.0 MeV. Based on this assumption, a 12 percent M/C fluence reduction (Reference 1) (i.e., not including the additional FERRET reduction) is applied to the DORT E > 1.0 MeV fluence prediction. The application of this M/C spectrum dependent correction is illustrated in Figure 6. While this conclusion may be correct, there are several other possible explanations for the observed 1.00/0.86 difference between the high/low-energy M/C biases that would not require this reduction in the DORT calculated fluence. These include: (1) the use of erroneously low dosimeter cross sections for Fe-54 and Ni-58 in the interpretation of the measurements, and/or (2) errors in the Fe-54 and Ni-58 measurements. (The number of U-238 and Np-237 dosimeters that are included in the in-vessel M/C bias is small and these measurements are subject to relatively large uncertainties.)

6.3 Least Squares Fluence Adjustment

The dosimetry measurements, transport calculations of the neutron flux and spectrum, and dosimetry cross sections include substantial uncertainties. The WCAP-14557 analysis uses the FERRET least squares adjustment method (Reference 18) to reduce the effect of these uncertainties on the fluence prediction. In this approach, the dosimeter measurements, dosimeter cross sections, and transport calculated neutron flux and spectrum are adjusted to obtain the optimum agreement, in the least squares sense, between the calculations and measurements. The adjustments made by FERRET are constrained by estimates of the magnitude and correlations of the uncertainties in these parameters. In the case of the Palisades fluence prediction, this adjustment results in about five percent reduction in the vessel fluence, in addition to the 12 percent reduction due to the application of the M/C bias. The adjusted fluence determined by FERRET is considered to be the best estimate fluence value.

A major concern with the application of the FERRET adjustment is that, while the adjustment does provide a best fit of the measured data, the dosimeter cross sections, measured reaction rates and calculated spectrum adjustments are made without any physical basis. This application of the FERRET adjustment methodology to Palisades is presently being evaluated and the results of this evaluation will be reported separately when completed.

6.4 Effect of Physical Plant Changes

The April 4, 1996, submittal included three physical changes to plant parameters which affect the calculated fluence value. The vessel inner radius was increased by 1/8 inches, the downcomer temperature was decreased by about 15° F, and the neutron source for the first five cycles was also increased. The results of the present calculations including the above changes, indicates an eight percent reduction to the peak fluence value compared to previously accepted value. Review of the proposed physical changes indicates that they are based on direct measurements, therefore, they are acceptable. The resulting reduction in the peak fluence value is likewise acceptable.

7.0 SUMMARY AND CONCLUSIONS

The licensee requested a 25 percent reduction to the pressure vessel fluence with respect to the value accepted in 1993. The request was based on: (1) changes of physical plant parameters (about an eight percent reduction); (2) a bias based on in vessel and reactor cavity dosimeter measurements (about 12 percent reduction); and (3) spectral adjustments of the measured values (about five percent reduction). Our review finds that: (1) the fluence reductions based on physical quantities to be acceptable, because they are based on directly measured parameters, (2) the 12 percent bias is not acceptable because the measurements are inconsistent and statistically incompatible, and (3) the spectral adjustments of five percent are not acceptable because they represent an intuitive averaging and do not evoke any physical principle. The spectral adjustments (five percent) are still under evaluation; however, it does not seem likely that the method is adequately justified.

The current fluence value for Palisades allows plant operation until 1999. The eight percent reduction will allow plant operation to about 2003. The current license for Palisades expires in 2007. If construction period recapture is requested, the license could be extended to 2011.

8.0 REFERENCES

1. DORT, Two-Dimensional Discrete Ordinates Transport Code, RSIC Computer Code Collection, CCC-484, Oak Ridge National Laboratory, 1988.

2. MESH - A Code for Determining the DOT Fixed Neutron Source, "BNL-Memorandum, M. D. Zentner to J. F. Carew, August 25, 1981.

3. Letter, Richard W. Smedley (CPC) to USNRC, Palisades Plant Updated Reactor Vessel Fluence Values, dated April 4, 1996.

4. 10 CFR 50.61 Pressurized Thermal Shock, Revised Projected Values of RT_{PTS} for Reactor Beltline Materials, Docket 50-255, June 10, 1993.

5. BNL Memorandum, J. F. Carew, K. Hu and A. Aronson to L. Lois, Palisades Pressure Vessel and Cavity Fluence Evaluation, dated March 15, 1994.

6. "Consumers Power Company Reactor Vessel Neutron Fluence Measurement Program for Palisades Nuclear Plant - Cycles 1 through 11," John D. Perock and Stanwood L. Anderson, WCAP-14557, March 1996.

7. Letter, John D. Perock (W) to John F. Carew (BNL), Transmittal of the Palisades Core Sources, dated June 21, 1996.

8. Letter, Richard W. Smedley (CPC) to USNRC, "Palisades Plant Updated Reactor Vessel Fluence Submittal - Additional Information," dated June 12, 1996.

9. Letter, Richard W. Smedley (CPC) to USNRC, "Palisades Plant Updated Reactor Vessel Fluence Submittal - Partial Response to Additional Questions," dated September 9, 1996.

10. Letter, Richard W. Smedley (CPC) to USNRC, Palisades Plant Updated Reactor Vessel Fluence Submittal - Partial Response to Additional Questions, dated September 19, 1996.

11. Letter, Thomas C. Bordine (CPC) to USNRC, "Palisades Plant Updated Reactor Vessel Fluence Submittal - Partial Response to Additional Questions," dated August 27, 1996.

12. Letter, J. F. Carew (BNL) to L. Lois (NRC), "Review of the Palisades Pressure Vessel Fluence Evaluation," dated July 19, 1996.

13. Production and Testing of the VITAMIN-B6 Fine Group and the BUGLE-93 Broad Group Neutron/Photon Cross-Section Libraries Derived from ENDF/B-VI Nuclear Data, D. T. Ingersoll, John E. White, Richard Q. Wright, Hamilton T. Hunter, Charles O. Slater, Robert E. MacFarlane, and Norman M. Greene, RSIC Data Library Collection, DLC-175, February 15, 1994.

14. The NJOY Nuclear Data Processing System, Volume I: Users Manual, R. E. MacFarlane, D. W. Muir, and R. M. Boicourt, LA-9303-M, Vol. I (ENDF-324), May 1982.

15. TRANSX:2.0 A Code for Interfacing MATXS Cross Section Libraries to Nuclear Transport Codes, R. E. MacFarlane, LA-12312-MS, Los Alamos National Laboratory, 1992.

16. Giant Resonance for the Actinide Nuclei: Photoneutron and Photofission Cross Sections for U-235, U-236, U-238 and Th-232, J. T. Cadwell, et. al, Physical Review, C2, 1973; and Very Low Energy Photofission of U-238, C. D. Bowman, et. al, Physical Review, C12, 1975.

17. Photofission and Photoneutron Cross Sections and Photofission and Photoneutron Multiplicities for U-233, U-234, Np-237 and Pu-239, B. L. Berman, et. al, Physical Review, C34, 2201, 1986.

18. "FERRET Data Analysis Code," E. A. Schmittroth, HEDL-TME-79-40, Hanford Engineering Laboratory, Richland, Washington, September 1979.

Table 1 Comparison of BNL and Westinghouse Palisades Calculated Fluence at Pressure Vessel Inner Wall Peak (E > 1.0 MeV)

Cycle	Cycle Length (EFPD)#	Fluence* ($\times 10^{18}$ neutron/cm^2*)		Ratio**
		BNL	W+	
1	379.4	1.569		
2	449.1	1.898		
3	349.5	1.664		
4	327.6	1.672		
5	394.6	1.974		
6	333.4	1.710		
7	369.9	1.806		
8	373.6	1.472		
9	298.5	0.7692		
10	356.9	0.6830		
11	430.4	0.7687		
Total		15.99	15.88	1.01

#Effective-Full-Power-Days.
*Fluences were taken at maximum azimuth.
**Ratio = Fluence (BNL)/Fluence (W).
+W cycle-specific values of the peak wall fluence were not available.

Table 2 BNL Palisades Fluence Calculation Uncertainty Analysis

Uncertainty Source	Fluence Sensitivity	Estimated Uncertainty	Fluence Uncertainty
1. PV Diameter	32% dF/in	0.12 in	3.8% dF
2. Core Neutron Source	1.0% dF/% ds	8% ds	8% dF
3. Nuclear Data			7% dF
4. Numerical Procedures			6% dF
5. Water Temperature: Core Core Bypass Down Comer	 0.25% dF/°F 0.37% dF/°F 0.36% dF/°F	 4°F 9°F 4°F	 1% dF 3.33% dF 1.44% dF
6. Others			5.0% dF
Total			14.2%

Table 3 Comparison of BNL and Westinghouse Dosimeter Reaction Rates (BNL/W)

Capsule	Cu-63 (n,α)	Ti-46 (n,p)	Fe-54 (n,p)	Ni-58 (n,p)	U-238 (n,f)	Np-237 (n,f)
W-290	1.00	1.07	1.01	1.02	1.02	*
W-110	1.00	1.05	1.00	1.01	*	*
16°/Cycle 8	0.97	1.06	1.01	1.02	1.04	1.06
16°/Cycle 9	0.98	1.06	1.03	1.02	1.04	1.06
16°/Cycles 10 and 11	0.97	0.90	0.94	0.94	0.92	0.91

Table 4 Comparison of BUGLE-93 and MATXS12 Calculations of the U-238 and Np-237 Dosimeter Photo-Fission Reaction Rate Contributions

Location	BUGLE-93 U-238(γ,f)/ U-238(n,f)	MATXS12 U-238(γ,f)/ U-238(n,f)	BUGLE-93 Np-237(γ,f)/ Np-237(n,f)	MATXS12 Np-237(γ,f)/ Np-237(n,f)
Vessel Inner-Wall	0.15	0.15	0.086	0.084
Cavity Inner-Wall	0.040	0.040	0.010	0.008

Table 5 Comparison of BNL(MATXS12) and Westinghouse Calculations of the U-238 and Np-237 Dosimeter Photo-Fission Reaction Rate Contributions

Location	BNL U-238(γ,f)/ U-238(n,f)	W U-238(γ,f)/ U-238(n,f)	BNL Np-237(γ,f)/ Np-237(n,f)	W Np-237(γ,f)/ Np-237(n,f)
Vessel Inner-Wall	0.15	0.11	0.084	0.069
Cavity	0.040	.037	0.008	0.008

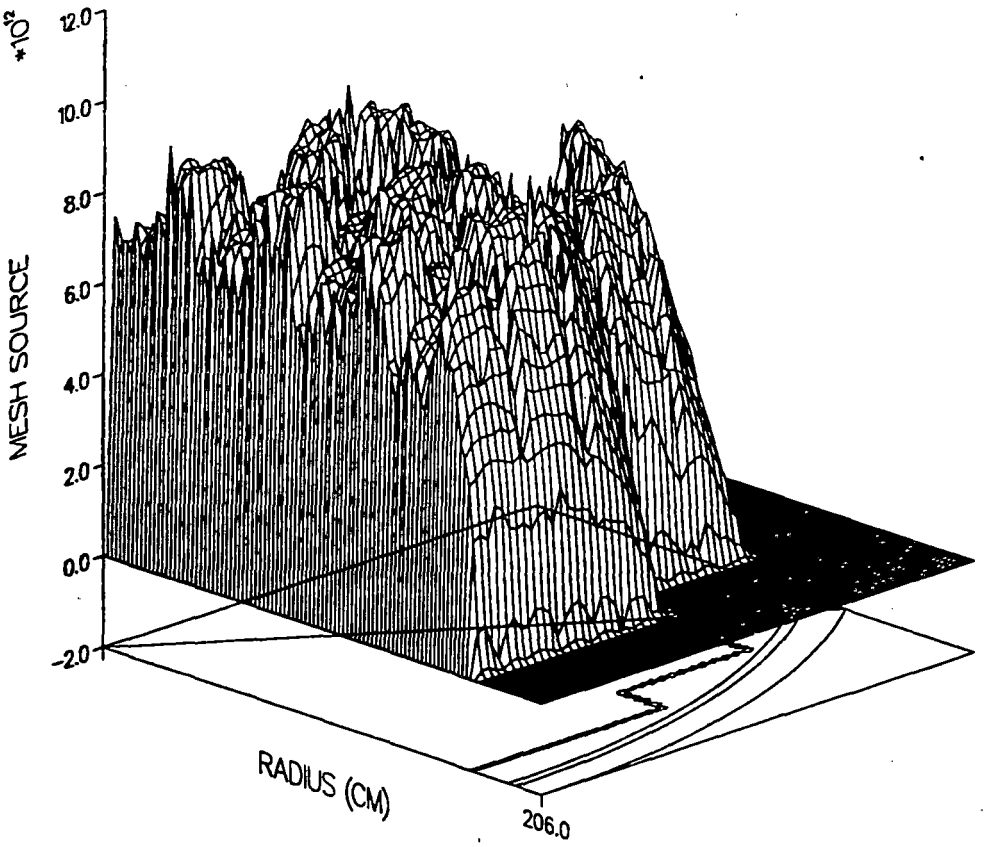

Figure 1 Palisades Cycle 1 Source

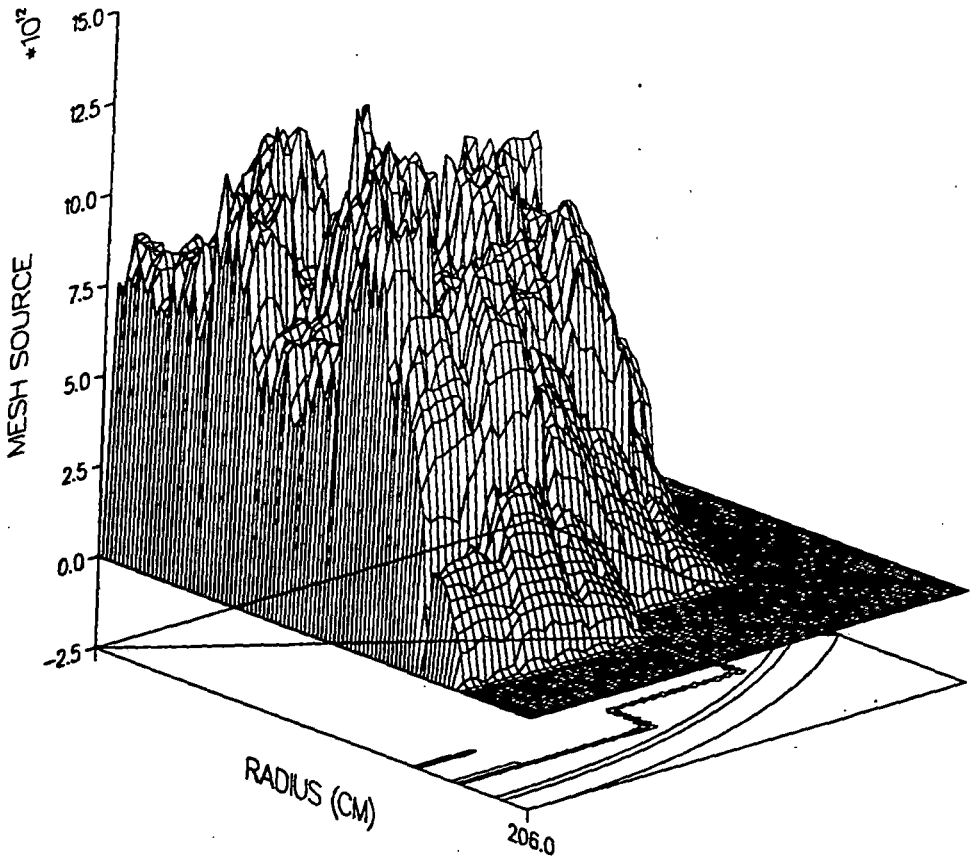

Figure 2 Palisades Cycle 11 Source

COMPARISON OF MEASURED AND CALCULATED NEUTRON SENSOR REACTION RATES FROM SURVEILLANCE CAPSULE AND CAVITY DOSIMETRY IRRADIATIONS

		High >4.0 MeV		Low <4.0 MeV			
		Cu63(n,α)	Ti46(n,p)	Fe54(n,p)	Ni58(n,p)	U238(n,f)	Np237(n,f)
In-Vessel	Internal						
	A240 (30°)	0.982	1.069	0.900	0.863		
	W290 (20°)	0.979	0.962	0.856	0.878	0.858	
	W290-9 (20°)	0.978	1.009	0.814	0.860	0.871	0.817
	W110 (20°)	0.997	0.993	0.852	0.865		
Cavity	6° Cavity						
	Cycle 8						
	Cycle 9	0.938	0.964	0.868	0.844	0.875	0.932
	Cycle 10/11	0.970	0.946	0.885	0.881	1.049	0.874
	16° Cavity						
	Cycle 8	0.904	0.948	0.854	0.852	0.833	1.083
	Cycle 9	0.883	0.911	0.821	0.830	0.753	0.900
	Cycle 10/11	0.934	0.930	0.853	0.874	0.868	0.864
	24° Cavity						
	Cycle 8						
	Cycle 9						
	Cycle 10/11	0.863	0.886	0.798	0.811	0.916	0.713
	26° Cavity						
	Cycle 8	0.887	0.933	0.830	0.825	0.797	0.992
	Cycle 9	0.896	0.919	0.815	0.834	0.873	0.982
	Cycle 10/11	0.910	0.943	0.849	0.838	0.885	0.888
	36° Cavity						
	Cycle 8						
	Cycle 9						
	Cycle 10/11	0.892	0.859	0.782		0.835	0.798
	39° Cavity						
	Cycle 8	0.922	0.940	0.840	0.822	0.771	0.934
	Cycle 9	0.891	0.896	0.794	0.798	0.708	0.752
	Cycle 10/11	0.845	0.908	0.808	0.810	0.814	0.793
	Average	0.922	0.942	0.836	0.843	0.847	0.880
	Std. Dev. (1σ)	0.046	0.049	0.033	0.026	0.079	0.101

Average Bias Factor (K)	0.879
Standard Deviation (1σ)	±0.072

Figure 3 M/C Reaction Rate Database

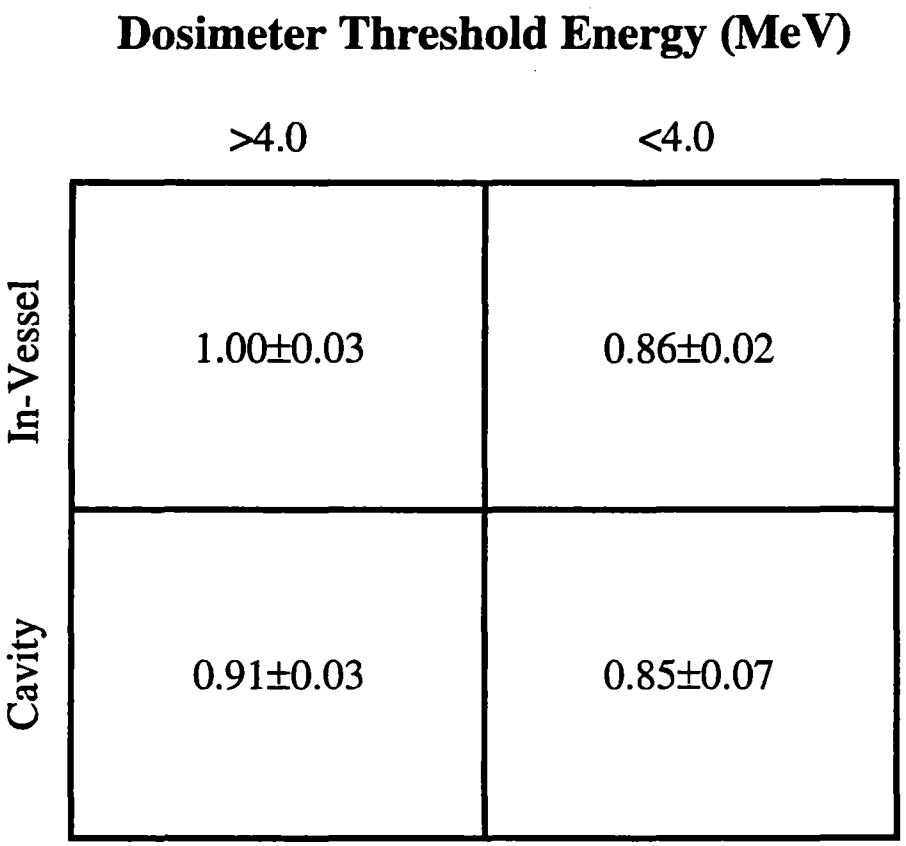

M/C Data Versus Location and Dosimeter Threshold Energy

Figure 4 Location and Energy Dependence of M/C Bias

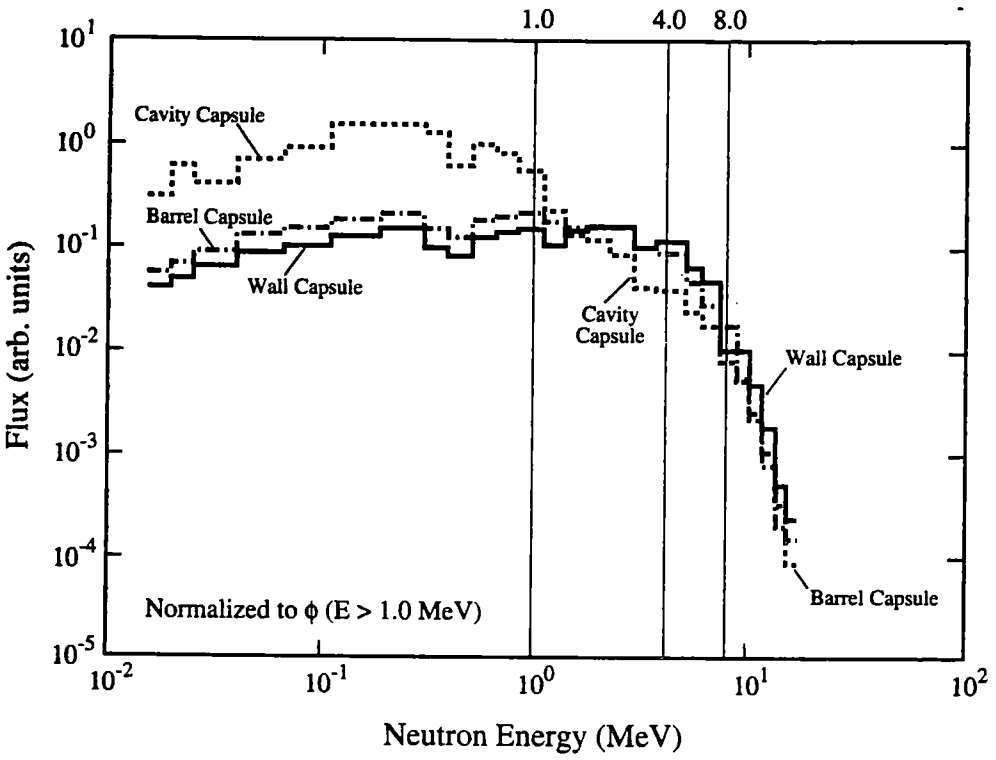

Figure 5 Spectral Dependence of Capsule Flux

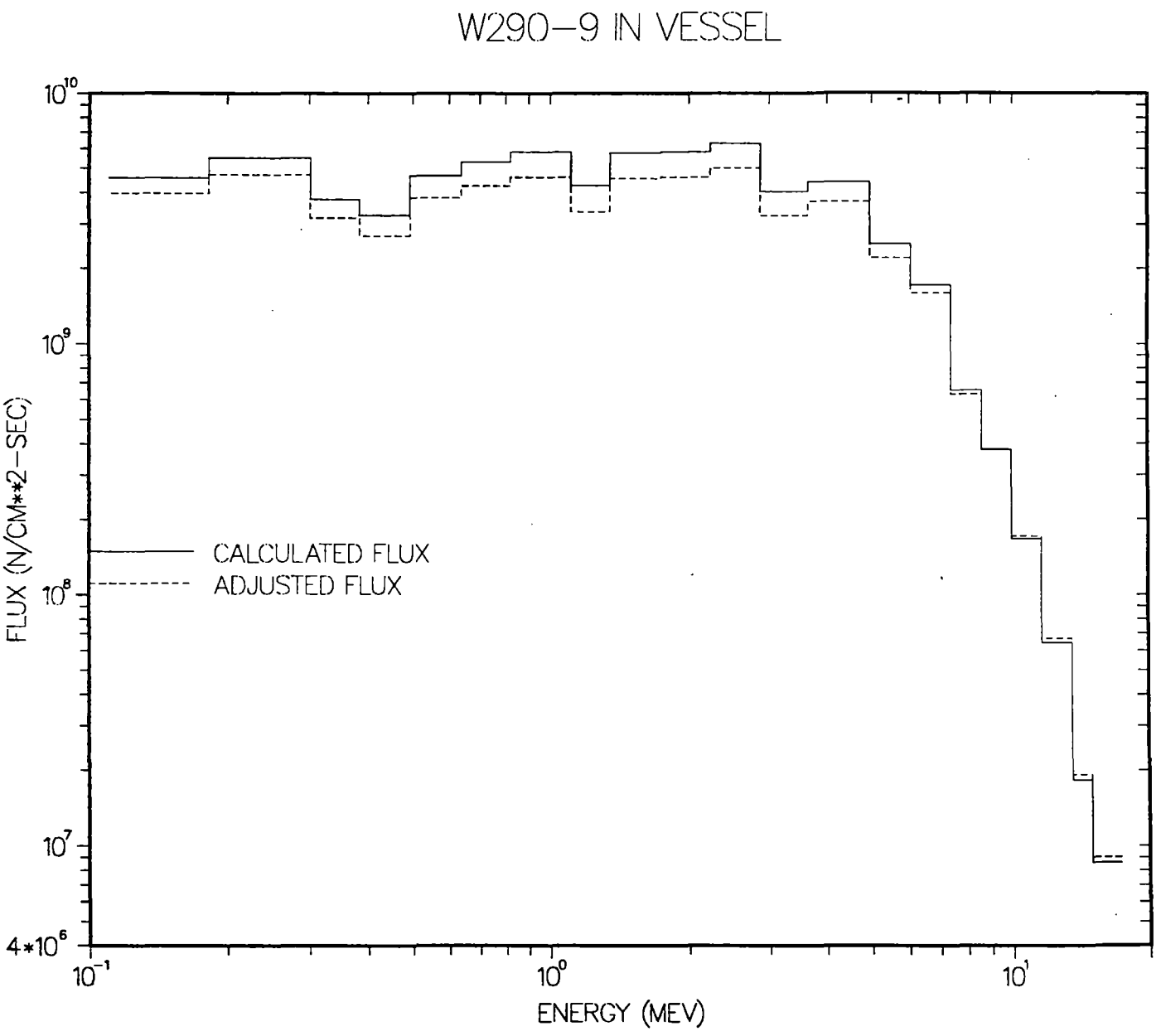

Figure 6 Capsule Flux Adjustment

BROOKHAVEN NATIONAL LABORATORY

M E M O R A N D U M

Safety & Risk Evaluation Division

DATE: November 15, 1996

TO: L. Lois

FROM: *J. F. Carew and A. Aronson*

SUBJECT: ***Palisades Cycles 1-11 Pressure Vessel and Cavity Fluence Evaluation***

I. Summary

Detailed calculations of the Palisades pressure vessel and cavity fluence for Cycles 1-11 have been carried out. The calculations use a pin-wise fuel exposure-dependent description of the core neutron source, and plant design and operating data provided by the Consumers Power Company (CPC) and Westinghouse (W). The calculations employ the DORT (Reference-1) discrete ordinates particle transport code and the MESH (Reference-2) source integration code, together with the BUGLE-93 ENDF/B-VI cross section data. The models include the recent (Reference-3) revisions to the Palisades plant data including the reduced downcomer/bypass temperatures, updated cycle-dependent pin-wise source and the increased vessel diameter and thickness. The BNL calculations indicate a Cycle-11 > 1-MeV vessel peak inner-wall fluence of 1.60×10^{19} n/cm^2, compared to the CPC/W calculation (prior to the application of the 0.83 measurement bias) of 1.59×10^{19} n/cm^2. An evaluation of uncertainties indicates a one-sigma uncertainty in these predictions of ~ 14%.

In order to evaluate the CPC/W interpretation of the U-238 and Np-237 fission dosimeters, coupled neutron/photon transport calculations of the Palisades dosimeter photo-fission contribution were also performed. These calculations indicate that the photo-fission contribution to the U-238(n,f) vessel-wall and cavity dosimeters is 15% and 4%, respectively, compared to the CPC/W values of 11% and 4%. The photo-fission contribution to the Np-237(n,f) vessel-wall and cavity dosimeters is calculated to be 8% and 1%, respectively, compared with the CPC/W predictions of 7% and 1%.

A review of the CPC/W application of the in-vessel and cavity measurements to the determination of the Palisades best-estimate fluence has also been performed. This review examined the Palisades measurement-to-calculation (M/C) data-base and the determination of the bias in the calculated fluence. The review indicated that the M/C data is not uniform and that certain important data

subsets exist for which the M/C calculational bias is significantly different than the M/C = 0.88 data-base average. The in-vessel high-energy and low-energy dosimeters indicate a substantial difference in M/C fluence bias; M/C = 1.0 ± .03 versus M/C = 0.86 ± .02, respectively. In the CPC/W analysis this difference is assumed to be due to a spectrum-dependent error in the DORT calculations which results in an exact calculation above E > 4.0 MeV and an overprediction for E < 4.0 MeV. Based on this assumption, a 12 % M/C fluence reduction is applied to the DORT E > 1.0 MeV fluence prediction. While this conclusion may be correct, several other possible explanations for the observed 1.00/0.86 difference between the high/low-energy M/C biases that would not require a reduction in the DORT calculated fluence are identified. These include: (1) the use of erroneously low dosimeter cross sections for Fe-54 and Ni-58 in the interpretation of the measurements and/or (2) errors in the Fe-54 and Ni-58 measurements.

II. Introduction

Consumers Power Company provided the evaluation of the Palisades pressure vessel peak wall fluence (PWF) through Cycle-9 in Reference-4 (June 1993). The BNL evaluation of this analysis (Reference-5) concluded that the CPC/W prediction of the Palisades vessel PWF was conservative. In the recent CPC submittal of Reference-3 (April 1996) entitled, "Palisades Plant Updated Reactor Vessel Fluence Values," the Reference-4 (1993) analysis is updated to include recent modeling improvements and the Cycle 10 and 11 cavity measurements. This updated fluence analysis takes credit for certain modeling conservatisms (e.g., reduced downcomer temperature and increased vessel diameter) and determines the best-estimate fluence value using a calculation-to-measurement bias. The combination of these changes in the Palisades fluence analysis results in an ~25% reduction in the predicted vessel fluence.

In the present analysis, under Task Order-12 of the Reactor Systems Branch Technical Assistance Program - Fin L-2589, an independent evaluation of the Palisades Cycle-11 vessel PWF is performed. The primary focus of this evaluation is: (1) the plant and source modeling and calculation of the vessel fluence, (2) the contribution of photo-fission to the U-238 and Np-237 dosimeter fluence measurements, (3) the uncertainty in the predicted fluence, and (4) the application of the measurements in determining the Palisades best-estimate fluence. The plant and source modeling were selected for detailed review since several of the identified conservatisms included in the Reference-3 updated analysis concerned the calculational models. The U-238 and Np-237 dosimeter measurements are used to adjust the calculated fluence and, since the photo-fission contribution to these dosimeters includes a substantial uncertainty, a detailed analysis of the photo-fission response was also performed. The application of the measurements was selected for review since the measurement renormalization results in a ~17% reduction in the Palisades fluence.

The methods used to calculate the vessel fluence and determine the dosimeter response in this analysis are consistent with the methods described in the Draft Regulatory Guide DG-1053. In performing this analysis a substantial effort was made to insure the use of the latest ENDF/B-VI nuclear cross section and fission spectra data. The required plant operating and design data including: (1) the geometry and material compositions of the core, internals, vessel and cavity, (2)

the cycle-dependent power and exposure distributions, (3) the operating temperatures and (4) the parameter uncertainties were obtained from Consumers Power and Westinghouse. The BNL calculational models are based on the information provided by CPC in the initial submittal (Reference 3) and attached WCAP-14557 Westinghouse Report (Reference-6), and in the subsequent (References 8-11) CPC responses to the Requests for Additional Information (RAIs) included in Reference-12. While these plant data were reviewed and generally found to be consistent and within expected limits, a detailed validation of the basic source data (e.g., verification of the temperature measurements, SIMULATE-3 depletion calculations and material composition specifications) was not performed.

The DORT discrete ordinates transport code was used to calculate the transport of the core neutron flux out to the vessel and into the cavity. The DORT calculations were performed for an axially-averaged horizontal plane in (r,θ) geometry. The MESH code was used to determine the space-energy dependent core neutron source in the required (r,θ) geometry for input to DORT. The calculations made use of the recent update to the MESH code to allow an accurate modeling of the core pin-wise power and source distributions in the individual fuel assemblies, and the stainless steel pins included in Cycles 8,10 and 11. Cycle-specific DORT calculations were performed for each cycle and then combined to determine the total accumulated vessel fluence through Cycle-11.

The calculational methods are described in the following Section III, the vessel fluence analysis is given in Section IV, the evaluation of the photo-fission contribution is given in Section V, and the evaluation of the application of the measurements to determine the best-estimate fluence is described in Section VI.

III. Calculational Methodology

III.1 Neutron Cross Sections and Fission Spectra

The Palisades fluence calculations were performed with the BUGLE-93 47-group neutron cross section library (Reference-13). The BUGLE-93 broad-group library was determined by collapsing the ENDF/B-VI VITAMIN-B6 171-group neutron/photon cross section set using spatially dependent spectra calculated for a typical PWR configuration. This library includes the recent updates to the iron, hydrogen, and oxygen cross sections, which together are known to result in a significant increase in the pressure vessel fluence prediction.

The fission spectra for U-235, U-238, Pu-239, Pu-240, Pu-241, and Pu-242 were used in the MESH calculations of the core neutron source. The ENDF/B-VI fission spectra for U-235, U-238, Pu-239, Pu-240, Pu-241, and Pu-242 were processed with NJOY (Reference-14). The surveillance capsule dosimeter reaction rates were calculated using the BUGLE-93 ENDF/B-VI cross sections.

III.2 Core Neutron Source

The calculation of the core neutron source includes the effect of the strong pin-wise variations of the power distribution in the fuel assemblies located near the core boundary. The cycle-dependent pin-wise power distribution for each assembly was provided in Reference-7. The MESH code was used to allocate the pin power to the individual (r,θ) mesh blocks. This allocation was performed by a numerical integration of the power distribution, defined on the (x,y) pin-wise mesh, over each (r,θ) mesh block. This numerical integration typically employed > 100 integration mesh per fuel pin and was shown to be accurate to within $< 1\%$ for each (r,θ) mesh block. As an example, the detailed core neutron source for Cycles 1 and 11 are given in Figures 1 and 2, respectively.

The magnitude of the core neutron source increases with fuel burnup due to the higher number of neutrons produced per MeV of energy by a Pu fission. This was taken into account by calculating the number of neutrons per MeV, ν/κ [neutrons/MeV], using fuel burnup dependent isotopic fission fractions. In addition, the fission spectrum was also considered to be dependent on the fuel burnup in order to account for the harder more penetrating neutron spectrum characteristic of the Pu fissions in the high-burnup fuel.

The group-dependent pin-wise source for each fuel assembly was determined for each cycle and used in the cycle-specific DORT calculations. The (r,θ) spatial mesh was modified in the MESH/DORT models to allow an accurate representation of the stainless steel pins that have been introduced in Cycles 8, 10 and 11 for flux-reduction.

III.3 Neutron Transport Calculations

The neutron transport calculations were performed with the ORNL DORT discrete ordinates transport code using the 47-group BUGLE-93 library. The calculations were performed in a fixed-source mode for a radial (r,θ) plane. The radial (r,θ) calculations were performed in a two-step "boot strap" fashion in which an inner one-eighth 45°-azimuthal sector was first calculated. A second outer one-eighth core 45°-azimuthal sector was then calculated using the flux on the inner surface of the annulus, calculated in the first inner calculation, as an input boundary condition. A ~ 15 cm radial overlap region between the inner and outer calculations was maintained to insure that the neglect of the outer geometry in the inner problem had a negligible effect (< 0.5%) on the vessel fluence calculations. The vessel axial peak was conservatively taken to be the same as the core axial power peak.

The calculations were performed using an S_8 quadrature and a P-3 angular decomposition of the scattering cross sections. The (r,θ) mesh included 61 angular mesh intervals, and 106 and 125 radial mesh intervals in the inner and outer bootstrap calculations, respectively. The angular (θ) and radial (r) mesh densities were increased at material interfaces where the geometry was changing rapidly, and at the capsule locations.

Vacuum boundary conditions were used on the outer radial and axial boundaries of the problems, and reflecting boundary conditions were used on the internal $\theta = 0°$ and $\theta = 45°$ azimuthal The boundaries. A pointwise flux convergence of 10^{-3} was used together with an integrated flux convergence criteria of 10^{-3}.

IV. Palisades Vessel Fluence and Surveillance Capsule Analysis

IV.1 Vessel Fluence Calculations

The pressure vessel peak wall fluence was calculated for each of the Palisades eleven operating cycles to account for the cycle-dependent changes in the downcomer temperatures, and to allow the determination of the surveillance capsule cycle-dependent reaction rates. The calculations include the increased vessel base metal thickness of 8.792 in., the increased vessel base metal inner radius of 86.35 in., the cycle-specific bypass and inlet temperatures based on the plant monitoring data, and the updated cycle-specific SIMULATE-3 pin-wise power distributions provided by CPC in Reference-4. The calculations include detailed modeling of the stainless steel replacement rods in the peripheral fuel assemblies as described in Reference-10, and the in-vessel surveillance capsule geometry as described in Reference-11.

The fluence was determined at the inner-wall of the vessel at the interface between the vessel clad and the base metal. The calculated fluence peak occurs at the 15.5° azimuth, opposite the corner assembly on the core flats. The calculated Palisades fluence is presented in Table-1 and indicates a peak > 1-MeV fluence of 1.60×10^{19} n/cm^2 at the vessel inner-wall at the end of Cycle-11. The fluence contribution and the cycle length (in effective-full-power days) for each cycle are also given in Table-1. For comparison, the Westinghouse (Reference-6) prediction of the peak wall fluence accumulated through Cycle-11 is 1.59×10^{19} n/cm^2. (The comparison of cycle-specific fluences is not made since the cycle values were not reported in Reference-6.) This Westinghouse fluence value does not include the 0.83 multiplicative adjustment that W applies to the calculated fluence to ensure agreement between the calculation and the Palisades measurements. This agreement between the BNL and W calculations (to within 1.0%) confirms the fluence prediction models and methods, and is well within the calculational uncertainties.

In order to estimate the uncertainty in the BNL > 1-MeV fluence prediction, a series of sensitivity calculations were performed for the known sources of significant uncertainty. In Table-2, these sensitivities are given along with the estimated (one-sigma) uncertainty components. The pressure vessel diameter uncertainty of ± 0.12 in. was provided by Consumers Power (Reference-11). The 8% source uncertainty (Item-2) is based, in part, on an estimate of the uncertainty in the peripheral assembly powers, and the (Item-5) water temperature uncertainties are based on expected reactor coolant system temperature calculation/measurement uncertainties. The nuclear data uncertainty estimate (Item-3) is based on expected data uncertainties and the numerical procedures uncertainty (Item-4) is based on the sensitivity of the fluence to numerical modeling and solution approximations. The other uncertainties included in Item-6 are relatively small model uncertainties that combine to add an additional 5% uncertainty to the total fluence. The total Palisades inner-wall > 1-MeV fluence uncertainty estimate is ± 14% (one-sigma).

IV.2 Surveillance Capsule Calculations

In the CPC/W methodology, the best-estimate fluence is determined by applying a multiplicative bias factor of 0.83 to the DORT calculation which results in a 17% reduction in the predicted fluence. This bias factor is based on a data-base of calculation-to-measurement comparisons made for the Palisades in-vessel and cavity surveillance capsules. As part of the evaluation of this procedure, calculations of several Palisades in-vessel and cavity capsule measurements were performed. The capsules calculated include: (1) the W-290 in-vessel capsule located at the 20° azimuth which was withdrawn after Cycle-5, (2) the W110 in-vessel capsule located at the 20° azimuth which was withdrawn after Cycle-10, and (3) the three cavity capsules located at the 16° azimuth which were irradiated during Cycle-8, Cycle-9, and Cycles 10 and 11. The capsules were

modeled in detail in the DORT calculations and were located at the positions given in Reference-6.

The reaction rates for these capsules were calculated for the Cu-63(n,α), Ti-46(n,p), Fe-54(n,p), Ni-58(n,p), U-238(n,f) and Np(n,f) reactions using the BUGLE-93 ENDF/B-VI dosimetry cross sections. The calculated reaction rates were compared to the CPC/W predictions for each capsule dosimeter and the results of this comparison are presented in Table-3. The agreement of the BNL and CPC/W predictions is generally good (to within a standard deviation of ~5%) and consistent with the good agreement observed between the > 1-MeV vessel fluence calculations of Table-1.

V. Evaluation of the Photo-Fission Contribution to the U-238(n,f) and Np-237(n,f) Dosimeters

The WCAP-14557 treatment of the photo-fission contribution to the U-238(n,f) and Np-237(n,f) dosimeters results in a reduction in the neutron fluence inferred from these measurements. This fluence reduction contributes directly to the 17% reduction (i.e., the 0.83 bias factor) in the Palisades best-estimate fluence. In view of the uncertainty associated with this contribution, a detailed analysis of the U-238 and Np-237 photo-fission effect was performed.

The determination of the photo-fission reaction requires the calculation of both the neutron and gamma flux. Since a significant fraction of the gamma flux is generated by low-energy thermal neutron captures, a cross section library with a reliable thermal-energy treatment is required. The CPC/W calculations were performed with the BUGLE-93 ENDF/B-VI cross section library which includes only two thermal neutron groups with no upscattering and is typically used for shielding applications rather than thermal neutron calculations. In order to provide an accurate treatment of the thermal neutron captures and a reliable gamma source, the MATXS12 ENDF/B-VI (Reference-15) coupled neutron/photon library was used for the calculation of the photo-fission contribution to the U-238 and Np-237 dosimeter responses. This cross section library is designed for light water thermal systems and includes forty-two thermal neutron groups and upscattering. For comparison, the calculations were also performed with the BUGLE-93 cross section library which was also used in the CPC/W calculations. The MATXS12 and BUGLE-93 (n,f) reaction rates were calculated using their respective dosimetry cross sections, and the U-238 and Np-237 photo-fission reaction rates were calculated using the cross sections of References 16 and 17, respectively.

The DORT coupled neutron/gamma transport calculations were performed using the detailed (r,θ) Palisades geometry. The BUGLE-93 calculations included 47-neutron groups and 20-gamma groups, and the MATXS12 calculations included 69-neutron groups and 24-gamma groups. The results of these calculations are presented in Table-4 and indicate that the BUGLE-93 and

MATXS12 predictions of the U-238(γ,f) and Np-237(γ,f) reaction rates are in good agreement for both the in-vessel and cavity capsules. The MATXS12 predictions are compared with the CPC/W predictions in Table-5 and indicate that the BNL and CPC/W photo-fission predictions are in good agreement. The comparisons indicate that: (1) the photo-fission correction is 15% and 4% for the U-238(n,f) dosimeter for the vessel inner-wall and cavity capsules, respectively and (2) the photo-fission correction is 8% and 1% for the Np-237 dosimeter for the vessel inner-wall and cavity capsules, respectively.

VI. Evaluation of Best-Estimate Fluence Determination

VI.1 Best-Estimate Fluence Determination

The best-estimate fluence determination of WCAP-14557 is made using the Palisades in-vessel and cavity measurements data-base. The Palisades measurements are compared to predictions of the dosimetry measurements made using the same codes and methods that are used to predict the vessel inner-wall fluence. Based on these measurement-to-calculation (M/C) comparisons of the dosimeter reaction rates, a M/C bias of 12 ($\pm$7)% is determined. This M/C bias is then adjusted using a least-squares adjustment technique to account for uncertainties in the measurements and calculations. In the case of Palisades this adjustment increases the M/C bias from 12% to 17%, and implies the calculations are overpredicting the fluence by 17%. The determination of the M/C bias and the adjustment method are discussed in the following sections.

VI.2 Fluence Calculation-to-Measurement Bias

The fluence measurement-to-calculation bias is based on the neutron dosimetry included in the accelerated surveillance capsule (A240) located on the outer-wall of the core support barrel, the three vessel inner-wall capsules (W290, W290-9 and W110), and the thirteen cavity measurements. The accelerated capsule was withdrawn after two cycles, the inner-wall capsules, A290 and W110, were withdrawn after Cycles 5 and 10, respectively, and Capsule A290-9 was only irradiated for Cycle-9. The cavity dosimetry included three azimuthal measurements for Cycle-8, four measurements for Cycle-9, and five measurements which were irradiated for both Cycles 10 and 11. All (except one) of the cavity measurements included the six dosimetry measurements; Cu-63(n,α), Ti-46(n,p), Fe-54(n,p), Ni-58 (n,p), U-238(n,f) and Np-237(n,f). The in-vessel dosimetry included all of these measurements except, in some cases, the U-238(n,f) and Np-237(n,f) dosimeters. The Palisades data-base included a total of ninety-six (96) measurement-to-calculation comparisons.

The measurement-to-calculation data-base used to determine the M/C = 0.88 fluence bias has been reviewed with respect to the consistency and reliability of the M/C data. The review was based on the material included in WCAP-14557 and the responses to the RAIs of References 4 and 8-11. The review concerned the measurement data-base since the analysis of Sections IV and V provided validation of the CPC/W fluence calculations. The primary focus was on: (1) the reliability of the M/C = 0.88 bias of Table 7.2-1 and (2) the applicability of this bias in determining a high confidence best-estimate value for the Palisades vessel fluence.

It is first noted that while the data-base includes random uncertainties due to the measurement process, these uncertainties contribute to the variability in the comparisons and are generally accounted for by the indicated ± 0.072 (one standard deviation) uncertainty in the calculated bias. The data-base included dosimeter reactions with product half-lives ranging from ~70 days to ~30 years which provided sensitivity to both the recent (few months) and long term (Cycles 1-11) fuel loading and operating history. However, the data-base did not indicate any significant dependence of the M/C bias on the dosimeter reaction half-life.

The Table 7.2-1 data-base consists of six dosimeter types which are measured for four in-vessel capsules and thirteen cavity capsules. The data-base includes a total of 96 M/C values which are averaged to determine the 12% fluence bias. The averaging of this data assumes that the M/C values represent samples drawn from the same underlying population. However, an examination of the data indicates that there are several subsets of the M/C data-base which have different M/C biases and appear to represent different distributions. For example, the M/Cs for the in-vessel dosimeters with thresholds greater than 4.0-MeV (viz., Cu-63 and Ti-46) indicate an M/C bias of $1.0 \pm .03$. The M/Cs for the cavity dosimeters with thresholds greater than 4.0-MeV indicate an M/C bias of $0.91 \pm .03$, and suggest a basic difference between the in-vessel and cavity M/Cs for the high energy dosimeters. In addition, the cavity dosimeters with thresholds less than 4.0-MeV indicate an M/C bias of $0.85 \pm .07$. This difference is important since 75% (77 out of 96) of the M/Cs are cavity measurements which yield the lowest fluence and, consequently, this data-base tends to maximize the fluence reduction.

The M/C bias indicates a significant dependence on the location of the dosimeters (cavity versus in-vessel) and on the energy threshold of the dosimeters ($E > 4.0$ MeV versus $E < 4.0$ MeV) as seen in Figures 3 and 4. In determining the measurement-to-calculation bias for the prediction of the inner-wall vessel fluence, it is important to recognize the difference in the fluence spectrum at these two locations. In Figure-5, a comparison of the fluence spectrum at the location of the accelerated (barrel outer-wall), the vessel inner-wall and the cavity capsules is presented. It is evident from this comparison that the fluence spectrum at the cavity capsule differs significantly from the spectrum at the vessel inner-wall where the fluence prediction is required. This is due, in part, to

the fact that Palisades does not have a thermal shield and the additional ~8" of steel between the inner-wall and cavity locations. It is concluded that the M/C comparisons made for the in-vessel dosimetry are a more accurate indication of the M/C to be used for the in-vessel fluence prediction.

From Figure-4, it is seen that the in-vessel M/C bias is 1.00 ±.03 for the dosimeters with thresholds E > 4.0 MeV, and 0.86 ± .02 for the dosimeters with thresholds E< 4.0 MeV. In the CPC/W analysis this difference is assumed to be due to a spectrum-dependent error in the DORT calculations which results in an exact calculation above E > 4.0 MeV and an overprediction for E < 4.0 MeV. Based on this assumption, a 12 % M/C fluence reduction[1] (i.e., not including the additional FERRET reduction) is applied to the DORT E > 1.0 MeV fluence prediction. The application of this M/C spectrum-dependent correction is illustrated in Figure-6. While this conclusion may be correct, there are several other possible explanations for the observed 1.00/0.86 difference between the high/low-energy M/C biases that would not require this reduction in the DORT calculated fluence. These include: (1) the use of erroneously low dosimeter cross sections for Fe-54 and Ni-58 in the interpretation of the measurements and/or (2) errors in the Fe-54 and Ni-58 measurements. (The number of U-238 and Np-237 dosimeters that are included in the in-vessel M/C bias is small and these measurements are subject to relatively large uncertainties).

IV.3 Least-Squares Fluence Adjustment

The dosimetry measurements, transport calculations of the neutron flux and spectrum, and dosimetry cross sections include substantial uncertainties. The WCAP-14557 analysis uses the FERRET least-squares adjustment method (Reference-18) to reduce the effect of these uncertainties on the fluence prediction. In this approach, the dosimeter measurements, dosimeter cross sections, and transport calculated neutron flux and spectrum are adjusted to obtain the optimum agreement, in the least-squares sense, between the calculations and measurements. The adjustments made by FERRET are constrained by estimates of the magnitude and correlations of the uncertainties in these parameters. In the case of the Palisades fluence prediction, this adjustment results in a ~5% reduction in the vessel fluence, in addition to the 12% reduction due to the application of the M/C bias. The adjusted fluence determined by FERRET is considered to be the best-estimate fluence value.

A major concern with the application of the FERRET adjustment is that, while the adjustment does provide a best-fit of the measured data, the dosimeter cross sections, measured reaction rates and calculated spectrum adjustments are made without any physical basis. This application of the FERRET adjustment methodology to Palisades is presently being evaluated and the results of this evaluation will be reported separately when completed.

References

1. "DORT, Two-Dimensional Discrete Ordinates Transport Code," RSIC Computer Code Collection, CCC-484, Oak Ridge National Laboratory, 1988.

2. "MESH - A Code for Determining the DOT Fixed Neutron Source," BNL-Memorandum, M. D. Zentner to J. F. Carew, August 25, 1981.

3. "Palisades Plant Updated Reactor Vessel Fluence Values," Letter, Richard W. Smedley (CPC) to USNRC, dated April 4, 1996.

4. "10 CFR 50.61 Pressurized Thermal Shock, Revised Projected Values of RT_{PTS} for Reactor Beltline Materials," Docket 50-255, June 10, 1993.

5. "Palisades Pressure Vessel and Cavity Fluence Evaluation," BNL-Memorandum, J. F. Carew, K. Hu and A. Aronson to L. Lois, Dated March 15, 1994.

6. "Consumers Power Company Reactor Vessel Neutron Fluence Measurement Program for Palisades Nuclear Plant - Cycles 1 through 11," John D. Perock and Stanwood L. Anderson, WCAP-14557, March 1996.

7. "Transmittal of the Palisades Core Sources," Letter, John D. Perock (W) to John F. Carew (BNL), Dated June 21, 1996.

8. "Palisades Plant Updated Reactor Vessel Fluence Submittal - Additional Information," Letter, Richard W. Smedley (CPC) to USNRC, Dated June 12, 1996.

9. "Palisades Plant Updated Reactor Vessel Fluence Submittal - Partial Response to Additional Questions," Letter, Richard W. Smedley (CPC) to USNRC, Dated September 9, 1996.

10. "Palisades Plant Updated Reactor Vessel Fluence Submittal - Partial Response to Additional Questions," Letter, Richard W. Smedley (CPC) to USNRC, Dated September 19, 1996.

11. "Palisades Plant Updated Reactor Vessel Fluence Submittal - Partial Response to Additional Questions," Letter, Thomas C. Bordine (CPC) to USNRC, Dated August 27, 1996.

12. "Review of the Palisades Pressure Vessel Fluence Evaluation," Letter, J. F. Carew (BNL) to L. Lois (NRC), Dated July 19, 1996.

13. "Production and Testing of the VITAMIN-B6 Fine Group and the BUGLE-93 Broad Group Neutron/Photon Cross-Section Libraries Derived from ENDF/B-VI Nuclear Data," D.T. Ingersoll, John E. White, Richard Q. Wright, Hamilton T. Hunter, Charles O. Slater, Robert E. MacFarlane, and Norman M. Greene, RSIC Data Library Collection, DLC-175, February 15, 1994.

14. "The NJOY Nuclear Data Processing System, Volume I: User's Manual," R. E. MacFarlane, D. W. Muir, and R. M. Boicourt, LA-9303-M, Vol. I (ENDF-324), May 1982.

15. "TRANSX:2.0 A Code for Interfacing MATXS Cross Section Libraries to Nuclear Transport Codes," R.E. MacFarlane, LA-12312-MS, Los Alamos National Laboratory, 1992.

16. "Giant Resonance for the Actinide Nuclei: Photoneutron and Photofission Cross Sections for U-235, U-236, U-238 and Th-232," J. T. Cadwell, et al., Physical Review, C2, 1973; and "Very Low Energy Photofission of U-238," C. D. Bowman, et al., Physical Review, C12, 1975.

17. "Photofission and Photoneutron Cross Sections and Photofission and Photoneutron Multiplicities for U-233, U-234, Np-237 and Pu-239," B.L. Berman, et al., Physical Review, C34, 2201, 1986.

18. "FERRET Data Analysis Code," E. A. Schmittroth, HEDL-TME-79-40, Hanford Engineering Laboratory, Richland, Washington, September 1979.

Table 1 Comparison of BNL and Westinghouse Palisades Fluence Calculations at Pressure Vessel Inner Wall Peak (E > 1.0 MeV)

Cycle	Cycle Length (EFPD)#	Fluence* ($\times 10^{18}$ neutron/cm^2*)		Ratio**
		BNL	W+	
1	379.4	1.569		
2	449.1	1.898		
3	349.5	1.664		
4	327.6	1.672		
5	394.6	1.974		
6	333.4	1.710		
7	369.9	1.806		
8	373.6	1.472		
9	298.5	0.7692		
10	356.9	0.6830		
11	430.4	0.7687		
Total		15.99	15.88	1.01

#Effective-Full-Power-Days.
*Fluences were taken at maximum azimuth.
**Ratio = Fluence (BNL)/Fluence (W).
+W cycle-specific values of the peak wall fluence were not available.

Table 2 BNL Palisades Fluence Calculation Uncertainty Analysis

Uncertainty Source	Fluence Sensitivity	Estimated Uncertainty	Fluence Uncertainty
1. PV Diameter	32% dF/in	0.12 in	3.8% dF
2. Core Neutron Source	1.0% dF/% ds	8% ds	8% dF
3. Nuclear Data			7% dF
4. Numerical Procedures			6% dF
5. Water Temperature: Core Bypass Down Comer	 0.25% dF/°F 0.37% dF/°F 0.36% dF/°F	 4°F 9°F 4°F	 1% dF 3.33% dF 1.44% dF
6. Others			5.0% dF
Total			14.2%

Table 3 Comparison of BNL and Westinghouse Dosimeter Reaction Rates (BNL/W)

Capsule	Cu-63 (n,α)	Ti-46 (n,p)	Fe-54 (n,p)	Ni-58 (n,p)	U-238 (n,f)	Np-237 (n,f)
W-290	1.00	1.07	1.01	1.02	1.02	*
W-110	1.00	1.05	1.00	1.01	*	*
16°/Cycle-8	0.97	1.06	1.01	1.02	1.04	1.06
16°/Cycle-9	0.98	1.06	1.03	1.02	1.04	1.06
16°/Cycle-10 and 11	0.97	0.90	0.94	0.94	0.92	0.91

Table 4 Comparison of BUGLE-93 and MATXS12 Calculations of the U-238 and Np-237 Dosimeter Photo-Fission Reaction Rate Contributions

Location	BUGLE-93 U-238(γ,f)/ U-238(n,f)	MATXS12 U-238(γ,f)/ U-238(n,f)	BUGLE-93 Np-237(γ,f)/ Np-237(n,f)	MATXS12 Np-237(γ,f)/ Np-237(n,f)
Vessel Inner-Wall	0.15	0.15	0.086	0.084
Cavity Inner-Wall	0.040	0.040	0.010	0.008

Table 5 Comparison of BNL(MATXS12) and Westinghouse Calculations of the U-238 and Np-237 Dosimeter Photo-Fission Reaction Rate Contributions

Location	BNL U-238(γ,f)/ U-238(n,f)	W U-238(γ,f)/ U-238(n,f)	BNL Np-237(γ,f)/ Np-237(n,f)	W Np-237(γ,f)/ Np-237(n,f)
Vessel Inner-Wall	0.15	0.11	0.084	0.069
Cavity Inner-Wall	0.040	.037	0.008	0.008

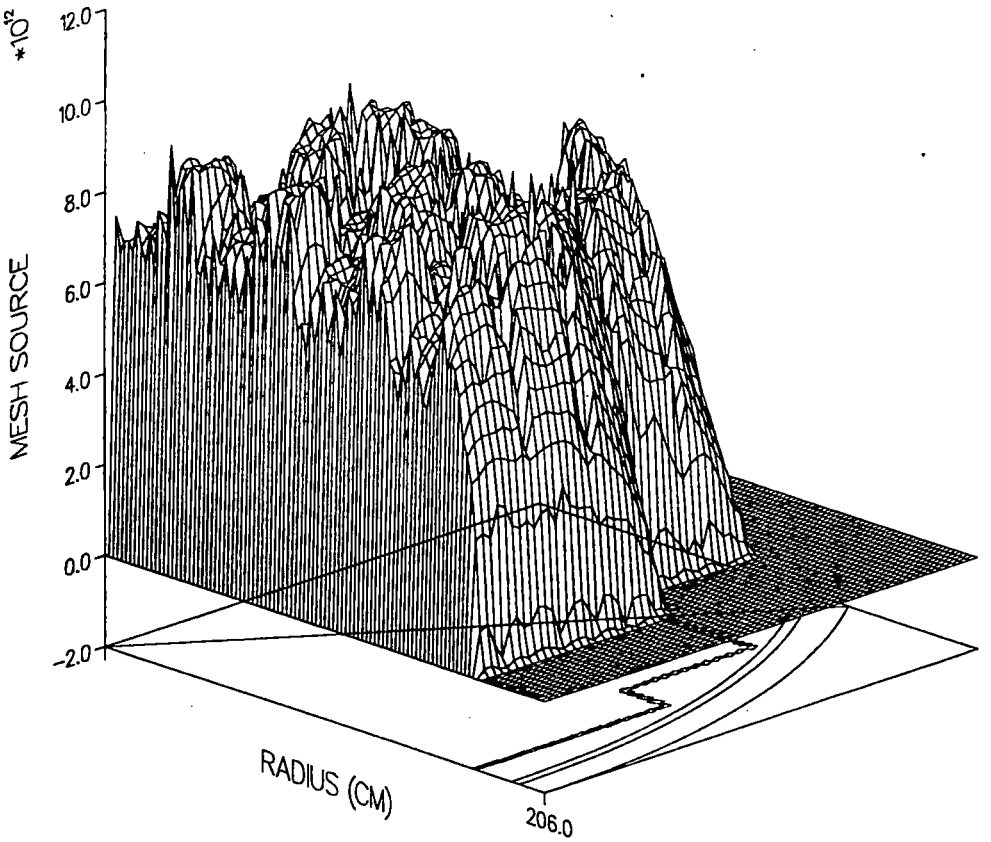

Figure 1 Palisades Cycle 1 Source

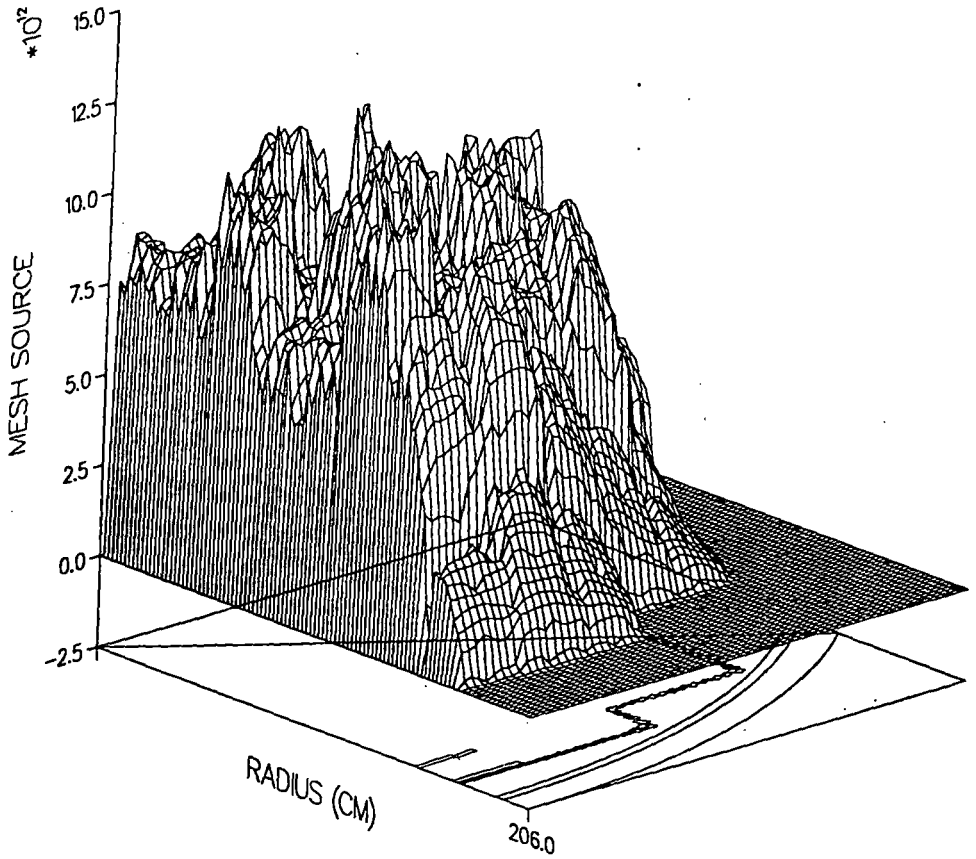

Figure 2 Palisades Cycle 11 Source

COMPARISON OF MEASURED AND CALCULATED NEUTRON SENSOR REACTION RATES FROM SURVEILLANCE CAPSULE AND CAVITY DOSIMETRY IRRADIATIONS

		High >4.0 MeV		Low <4.0 MeV			
		Cu63(n,α)	Ti46(n,p)	Fe54(n,p)	Ni58(n,p)	U238(n,f)	Np237(n,f)
In-Vessel	Internal						
	A240 (30°)	0.982	1.069	0.900	0.863		
	W290 (20°)	0.979	0.962	0.856	0.878	0.858	
	W290-9 (20°)	0.978	1.009	0.814	0.860	0.871	0.817
	W110 (20°)	0.997	0.993	0.852	0.865		
Cavity	6° Cavity						
	Cycle 8						
	Cycle 9	0.938	0.964	0.868	0.844	0.875	0.932
	Cycle 10/11	0.970	0.946	0.885	0.881	1.049	0.874
	16° Cavity						
	Cycle 8	0.904	0.948	0.854	0.852	0.833	1.083
	Cycle 9	0.883	0.911	0.821	0.830	0.753	0.900
	Cycle 10/11	0.934	0.930	0.853	0.874	0.868	0.864
	24° Cavity						
	Cycle 8						
	Cycle 9						
	Cycle 10/11	0.863	0.886	0.798	0.811	0.916	0.713
	26° Cavity						
	Cycle 8	0.887	0.933	0.830	0.825	0.797	0.992
	Cycle 9	0.896	0.919	0.815	0.834	0.873	0.982
	Cycle 10/11	0.910	0.943	0.849	0.838	0.885	0.888
	36° Cavity						
	Cycle 8						
	Cycle 9						
	Cycle 10/11	0.892	0.859	0.782		0.835	0.798
	39° Cavity						
	Cycle 8	0.922	0.940	0.840	0.822	0.771	0.934
	Cycle 9	0.891	0.896	0.794	0.798	0.708	0.752
	Cycle 10/11	0.845	0.908	0.808	0.810	0.814	0.793
	Average	0.922	0.942	0.836	0.843	0.847	0.880
	Std. Dev. (1σ)	0.046	0.049	0.033	0.026	0.079	0.101

Average Bias Factor (K)	0.879
Standard Deviation (1σ)	±0.072

Figure 3 M/C Reaction Rate Database

Dosimeter Threshold Energy (MeV)

	>4.0	<4.0
In-Vessel	1.00±0.03	0.86±0.02
Cavity	0.91±0.03	0.85±0.07

M/C Data Versus Location and Dosimeter Threshold Energy

Figure 4 Location and Energy Dependence of M/C Bias

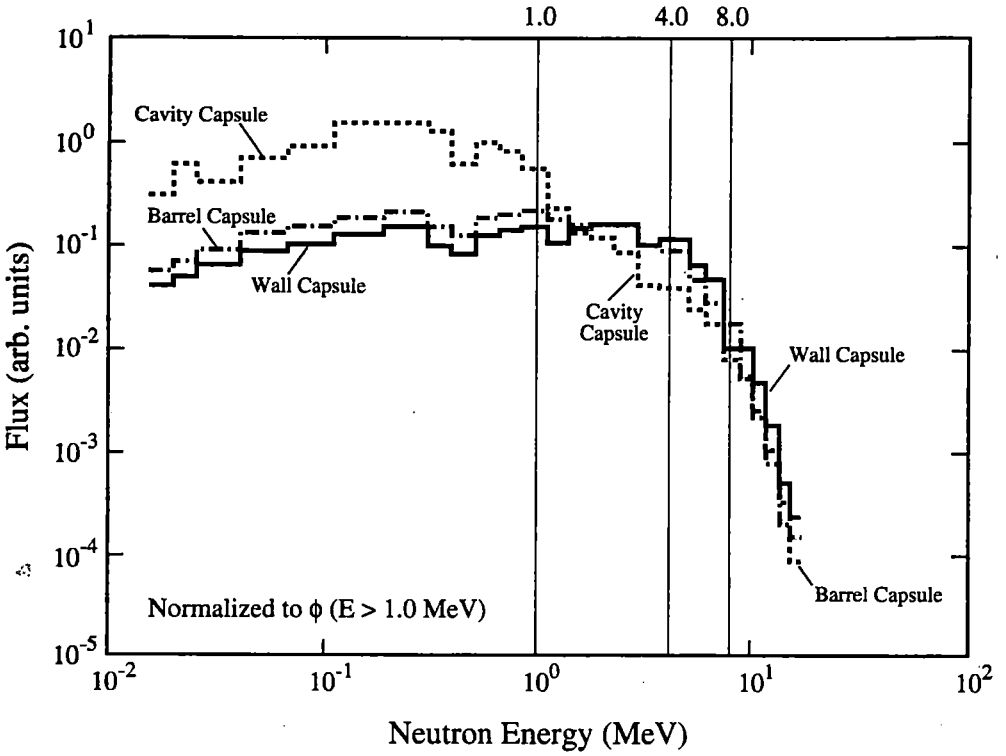

Figure 5 Spectral Dependence of Capsule Flux

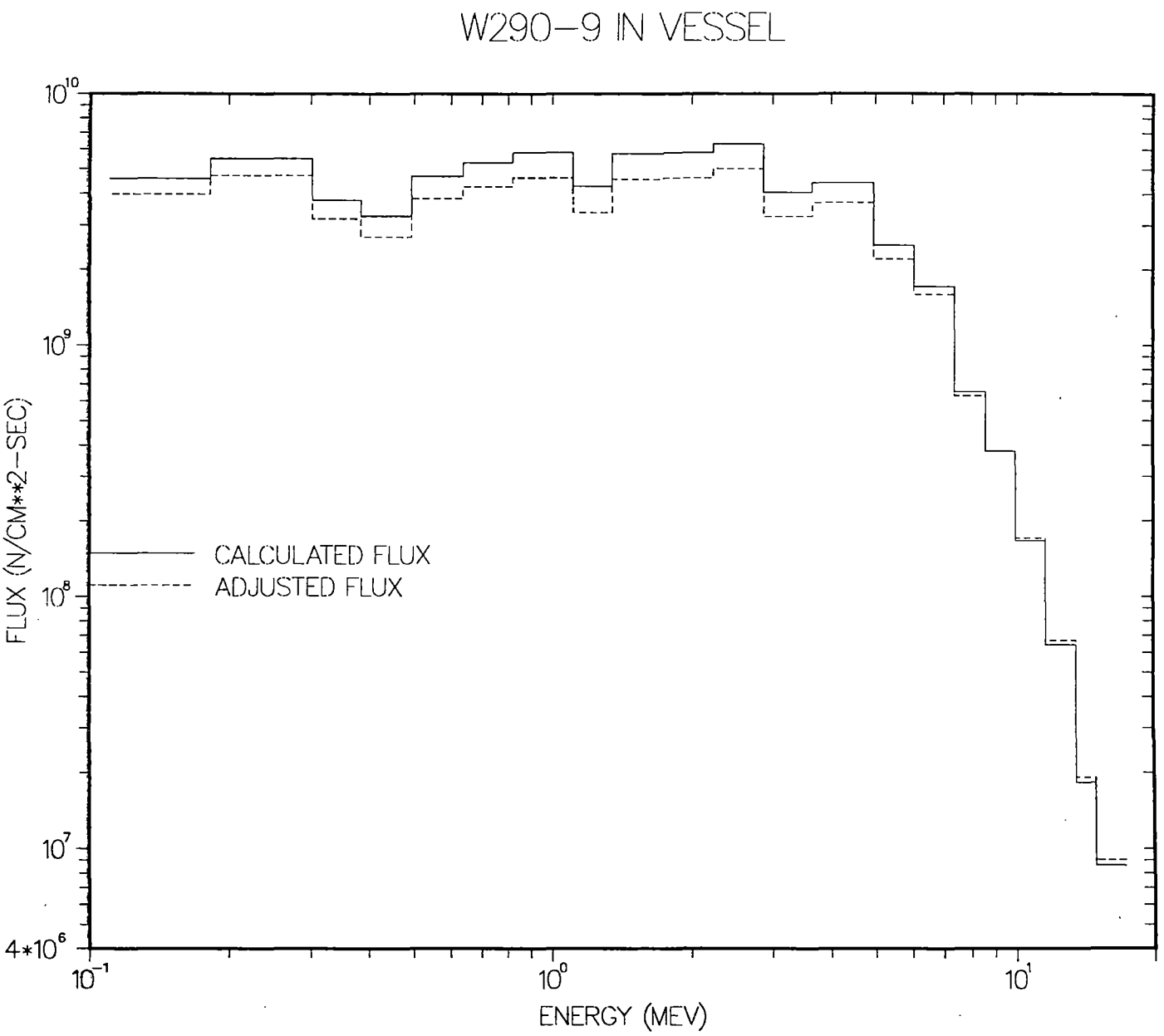

Figure 6 Capsule Flux Adjustment